

# Retroviral insertional mutagenesis identifies *Zeb2* activation as a novel leukemogenic collaborating event in *CALM-AF10* transgenic mice

\*David Caudell,<sup>1,2</sup> \*David P. Harper,<sup>2,3</sup> Rachel L. Novak,<sup>2</sup> Rachel M. Pierce,<sup>2</sup> Christopher Slape,<sup>4</sup> Linda Wolff,<sup>5</sup> and Peter D. Aplan<sup>2</sup>

<sup>1</sup>Department of Biomedical Sciences and Pathobiology, Center for Molecular Medicine and Infectious Diseases, Virginia-Maryland College of Veterinary Medicine, Virginia Tech, Blacksburg; <sup>2</sup>Genetics Branch, Center for Cancer Research, National Cancer Institute, National Institute of Health, Bethesda, MD; <sup>3</sup>Department of Pediatrics, Uniformed Services University of the Health Sciences, Bethesda, MD; <sup>4</sup>Bone Marrow Research Laboratory, Royal Melbourne Hospital, Parkville, Australia; and <sup>5</sup>Laboratory of Cellular Oncology, Center for Cancer Research, National Cancer Institute, National Institutes of Health, Bethesda, MD

The t(10;11) translocation results in a *CALM-AF10* fusion gene in a subset of leukemia patients. Expression of a *CALM-AF10* transgene results in leukemia, with prolonged latency and incomplete penetrance, suggesting that additional events are necessary for leukemic transformation. *CALM-AF10* mice infected with the MOL407LTR retrovirus developed acute leukemia, and ligation-mediated polymerase chain reaction was used to identify retroviral insertions at 19 common insertion sites, including

*Zeb2*, *Nf1*, *Mn1*, *Evi1*, *Ift57*, *Mpl*, *Plag1*, *Kras*, *Erg*, *Vav1*, and *Gata1*. A total of 26% (11 of 42) of the mice had retroviral integrations near *Zeb2*, a transcriptional corepressor leading to overexpression of the *Zeb2*-transcript. A total of 91% (10 of 11) of mice with *Zeb2* insertions developed B-lineage acute lymphoblastic leukemia, suggesting that *Zeb2* activation promotes the transformation of *CALM-AF10* hematopoietic precursors toward B-lineage leukemias. More than half of the mice with

*Zeb2* integrations also had *Nf1* integrations, suggesting cooperativity among *CALM-AF10*, *Zeb2*, and *Ras* pathway mutations. We searched for *Nras*, *Kras*, and *Ptpn11* point mutations in the *CALM-AF10* leukemic mice. Three mutations were identified, all of which occurred in mice with *Zeb2* integrations, consistent with the hypothesis that *Zeb2* and *Ras* pathway activation promotes B-lineage leukemic transformation in concert with *CALM-AF10*. (Blood. 2010; 115:1194-1203)

## Introduction

The rare but recurring chromosomal translocation t(10;11)(p12;q14) results in a *CALM-AF10* fusion that is present in patients with both acute lymphoblastic leukemia (ALL) and acute myeloid leukemia (AML).<sup>1-3</sup> Using murine retroviral transduction and transplantation, Deshpande et al demonstrated that expression of a *CALM-AF10* fusion led to AML with B-lymphoid characteristics.<sup>4</sup> Subsequently, we demonstrated that mice that express a *CALM-AF10* transgene in the hematopoietic compartment develop AML with lymphoid (both B-cell and T-cell) features.<sup>5</sup> In general, these mice developed leukemia after a long latency period (median, 12 months) with incomplete penetrance (40%-50%). These findings suggest that additional genetic events are needed to complement the leukemogenic effect of the *CALM-AF10* transgene, and are consistent with an emerging paradigm, which predicts that most, if not all, leukemic cells must undergo at least 2 collaborative oncogenic events to produce a malignant cell.<sup>6</sup> As a consequence of these cumulative genetic and epigenetic events, the affected cell has a clonal advantage and progresses to a fully malignant cell.

Spectral karyotyping, comparative genomic hybridization, retroviral insertional mutagenesis, and targeted resequencing have been used to detect collaborative mutations associated with cancer.<sup>7,8</sup> Retroviral insertional mutagenesis (RIM) is a whole-genome screening technique used to identify cancer-associated

genes, including those involved in hematopoietic malignancies.<sup>9</sup> Infection of murine hematopoietic cells with a retrovirus allows for integration of the viral DNA (provirus) into the host genome. Insertion of the provirus can lead to cellular transformation by several mechanisms, including activation of proto-oncogenes by viral long terminal repeats (LTRs), which can enhance transcription of nearby genes, or inactivation of tumor suppressor genes, through disruption of coding sequences.<sup>10</sup> Dysregulation of proto-oncogenes and tumor suppressor genes results in a growth advantage and clonal expansion of transformed cells. Genes influenced by proviral integration can be identified through ligation-mediated polymerase chain reaction (LM-PCR) using viral sequence as PCR primers.

Because of the long latency period and incomplete penetrance observed in our initial *CALM-AF10* study,<sup>5</sup> we hypothesized that retroviral infection would accelerate the leukemia and allow us to identify genes that collaborate with the *CALM-AF10* transgene. In addition, the 2 most differentially expressed genes in *CALM-AF10* bone marrow (BM) are *Meis1* and *Hoxa9*<sup>5</sup> (D.C., R.L.N., and P.D.A., unpublished data, June 2008). In this context, it is important to note that overexpression of *HOXA* cluster genes, particularly *HOXA9* and *MEIS1*, is a common finding in both AML<sup>11</sup> as well as B-lineage ALL associated with *MLL* fusions.<sup>12</sup> Therefore, we speculated that the leukemias that develop in

Submitted April 10, 2009; accepted November 10, 2009. Prepublished online as *Blood* First Edition paper, December 9, 2009; DOI 10.1182/blood-2009-04-216184.

\*D.C. and D.P.H. contributed equally to this study.

The online version of this article contains a data supplement.

The publication costs of this article were defrayed in part by page charge payment. Therefore, and solely to indicate this fact, this article is hereby marked "advertisement" in accordance with 18 USC section 1734.

*CALM-AF10* mice might identify genes that collaborate with other leukemias that overexpress *MEIS1* and *HOXA9*, such as those associated with *MLL* fusions.

The MOL4070LTR is a recombinant retrovirus, derived from the Moloney murine leukemia virus and the 4070A virus, which has been shown to cause myeloid leukemia in approximately half of the infected mice, in contrast to Moloney murine leukemia virus, which is associated with a predominantly lymphoid phenotype.<sup>13</sup> Using the MOL4070LTR virus, we show that retroviral insertional mutagenesis accelerates the onset of acute leukemia in *CALM-AF10* transgenic mice and identifies genes that potentially collaborate with the *CALM-AF10* fusion gene during leukemic transformation.

## Methods

### Retroviral infection

The MOL4070LTR retrovirus was propagated and virus harvested as described.<sup>13</sup> Newborn *CALM-AF10* transgenic and wild-type (WT) mice were inoculated intraperitoneally with  $4 \times 10^4$  infectious particles. All animal experiments were conducted with the approval of the National Institutes of Health Intramural Animal Care and Use Committee.

### Pathologic evaluation and immunophenotype

Mice were observed daily for signs of leukemia and killed when symptomatic. BM was harvested by flushing femora with Dulbecco medium containing 2% fetal calf serum (Invitrogen), hereafter referred to as HF2. Blood smears and cytospins were stained with May-Grunwald-Giemsa (Sigma-Aldrich). Tissues were fixed in 10% neutral buffered formalin (Sigma-Aldrich), paraffin embedded, sectioned, and stained with hematoxylin and eosin or incubated with the following monoclonal antibodies: antimyeloperoxidase (Dako North America), anti-CD3 (Dako North America), F4/80 (Caltag), and B220 (CD45R; BD Biosciences PharMingen). Single-cell suspensions from spleen and/or BM were incubated with fluorescein isothiocyanate-conjugated anti-mouse CD8, B220, and Gr1 or phycoerythrin-conjugated anti-mouse CD4 and CD11b (Mac1; BD Biosciences PharMingen) and analyzed by flow cytometry. Leukemias were classified according to the Bethesda proposals.<sup>14,15</sup> Photomicrographs were taken on a BX51 Olympus microscope (Olympus America) with an Olympus DP12 camera system using 20 $\times$  and 100 $\times$  objectives and a 10 $\times$  eyepiece objective. Digital images were imported into PowerPoint (Microsoft).

### LM-PCR

Retroviral integration sites were cloned using LM-PCR.<sup>16</sup> PCR products were purified (QIAGEN), ligated into pGEM-T Easy (Promega), and transformed into DH5 $\alpha$  *Escherichia coli* cells (Invitrogen). Plasmid DNA was isolated and sequenced (Retrogen). Sequences were compared with National Center for Biotechnology Information mouse genome Build 36 (February 2006) using the UCSC genome browser (<http://genome.ucsc.edu/>).

### Southern blot analysis

Genomic DNA from leukemic spleens was digested with *EcoRI* (for virus integrations or *Igh* gene rearrangements), *XbaI* (for *Igh* gene rearrangements), *SmaI* (for *Zeb2* gene rearrangements), *BamHI* or *HindIII* (for *Nf1* gene rearrangements), size fractionated on agarose gels, denatured, neutralized, and transferred to nylon membranes (Schliecher & Schuell). The nylon membranes were hybridized (Ultrascreen; Ambion) to PCR-generated probes for either MOL4070LTR envelope, murine *Zeb2*, or murine *Nf1*. The murine *Igh* probe was a gift from Michael Kuehl (National Cancer Institute). Probes were labeled with <sup>32</sup>P using Amersham Ready-To-Go DNA Labeling Beads (GE Healthcare). Primer sequences used to generate the murine *Zeb2* and murine *Nf1* probes are in supplemental Table 1 (available on the Blood website; see the Supplemental Materials link at the top of the online article).

### Western blot analysis

Spleens were lysed in RIPA (Radio-immunoprecipitation assay) buffer (1 $\times$  Tris-buffered saline, 1% NP-40, 0.5% sodium deoxycholate, 0.1% sodium dodecyl sulfate, 0.004% sodium azide) supplemented with complete protease inhibitor cocktail (0.2mM phenylmethanesulfonyl fluoride and 0.1mM sodium orthovanadate; Santa Cruz Biotechnology) on ice for 30 minutes. Total protein (30  $\mu$ g) was diluted in 2 $\times$  sample buffer, boiled for 10 minutes, resolved on 6% and 10% Tris-glycine gels (Invitrogen), and transferred to nitrocellulose membranes (Invitrogen). Membranes were blocked with 1 $\times$  Tris-buffered saline containing 0.1% Tween-20 (TBST) and 5% skim milk for 60 minutes at room temperature, and incubated with an anti-Nf1 murine monoclonal antibody (1:1000, McNFn27; Santa Cruz Biotechnology) or anti- $\alpha$ -tubulin rabbit polyclonal antibody (1:1000; Cell Signaling). Membranes were washed 3 times for 15 minutes in TBST at room temperature followed by a 60-minute incubation with horseradish peroxidase-conjugated anti-mouse or anti-rabbit antibodies (Pierce Chemical). Finally, the membranes were washed 3 times for 15 minutes each in TBST at room temperature and incubated with Enhanced Chemiluminescence solution (Pierce Chemical). Band intensity was quantified with ImageJ software (National Institutes of Health).

### Real-time quantitative PCR

Total RNA was isolated using TRIzol (Invitrogen); 1  $\mu$ g was reverse transcribed with *Superscript II* reverse transcriptase and random hexamer primers (Invitrogen) in 20- $\mu$ L reactions. Real-time reverse transcription PCR (RT-PCR) was performed on a 7500 Fast Real-Time TaqMan PCR system (Applied Biosystems) using aliquots of 1  $\mu$ L from the first-strand cDNA as templates. TaqMan primer and probes sets were purchased from Applied Biosystems (supplemental Table 1). All reactions were in triplicate with 20- $\mu$ L PCR reactions using Applied Biosystems default thermal cycling conditions. The  $-\Delta\Delta C_T$  mean and SE were calculated for each sample and normalized to the 18S rRNA value.

### ZEB2 knockdown with siRNA

B-ALL1 (gift of David Chervinsky, Roswell Park Cancer Institute) and MV4-11 (ATCC) cell lines were cultured in Iscove modified Dulbecco medium (IMDM) media (Invitrogen) supplemented with 15% fetal bovine serum, 10  $\mu$ g/mL penicillin/streptomycin, and 100mM L-glutamine (Invitrogen). A total of  $3 \times 10^5$  MV4-11 or B-ALL1 cells were seeded in 100  $\mu$ L of serum-free IMDM. A total of 1.5  $\mu$ g of small interfering RNA (siRNA) specific to human *ZEB2* or a nonspecific siRNA control (QIAGEN) was mixed with 6  $\mu$ L of HiPerFect transfection reagent (QIAGEN) in 100  $\mu$ L of serum-free IMDM and incubated at room temperature for 10 minutes. The siRNA/lipid complexes were added to the cells and incubated at 37 $^\circ$ C for 6 hours. Next, 600  $\mu$ L of complete IMDM was added, and the cells were incubated at 37 $^\circ$ C/5% CO<sub>2</sub>. At 24, 48, and 120 hours after transfection, cell numbers were determined by hemocytometer. Transfections were performed in triplicate, and the mean cell number and SD for each time point were determined. For quantitative RT-PCR analysis of *ZEB2* expression, cells were harvested in Trizol (Invitrogen) at 24 hours after transfection and analyzed by quantitative RT-PCR as described in "Real-time quantitative PCR."

### Resequencing

Genomic DNA from leukemic spleens was amplified using primers listed in supplemental Table 1. PCR cycling conditions were: 94 $^\circ$ C for 3 minutes, 40 cycles of 94 $^\circ$ C for 30 seconds, 63 $^\circ$ C (57 $^\circ$ C for *Kras* exon 2 and 64.5 $^\circ$ C for *Nras* exon 3) for 30 seconds, and 72 $^\circ$ C for 60 seconds, followed by 72 $^\circ$ C for 5 minutes. PCR products were purified using QIAGEN reagents and protocols and directly sequenced (Retrogen). Sequence chromatograms were manually evaluated for evidence of mutations.

### Statistical analysis

Statistical significance for survival data was tested using the log-rank (Mantel-Cox) test; data for quantitative RT-PCR are expressed as mean plus or minus SD and were tested using an unpaired Student *t* test; data for

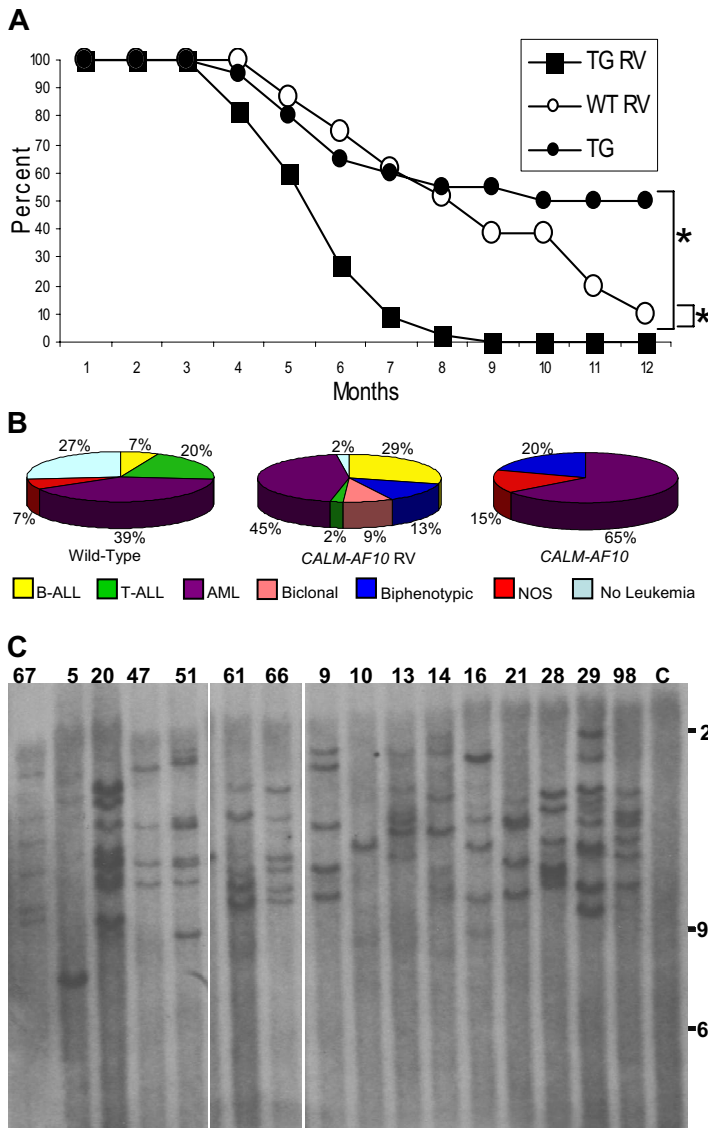


**Figure 1. MOL4070LTR infection accelerates leukemic transformation in *CALM-AF10* mice.** (A) Survival of MOL4070LTR-infected *CALM-AF10* mice (■, N = 45), MOL4070LTR-infected WT (○, n = 31), and noninfected *CALM-AF10* transgenic mice (●, N = 20). \* $P < .001$ , comparing infected *CALM-AF10* transgenic mice with noninfected *CALM-AF10*, or infected *CALM-AF10* with WT mice using a log-rank test. (B) Distribution of leukemia by immunophenotype in WT and *CALM-AF10* mice infected with MOL4070LTR retrovirus. Note the predominance of B-cell and myeloid (AML) tumors, as well as the lack of pre-T LBL, in the *CALM-AF10* mice compared with the WT control mice. (C) Retroviral integration analysis. Southern blot of *EcoRI*-digested DNA extracted from leukemic spleens hybridized to a viral *env* probe. Mouse identification numbers are indicated; C indicates germline control tissue; size standards are given in kilobases. The proviral genome is 8.7 kb and does not contain an *EcoRI* site.

relative expression by expression array are expressed as mean plus or minus SD, and groups are compared using an unpaired Student *t* test using GraphPad Prism, Version 5.00 for Windows (GraphPad Software). Data for genotype/phenotype and genotype/genotype correlations were tested using Fisher exact test.

## Results

### MOL4070LTR infection accelerates the onset of acute leukemia in *CALM-AF10* transgenic mice

A total of 45 *CALM-AF10* and 31 WT littermate control mice were infected at birth and monitored for signs of leukemia. Acute leukemia developed more rapidly in *CALM-AF10*-infected mice than in either the FVB WT mice infected with retrovirus ( $P < .001$ ) or *CALM-AF10* mice not infected with retrovirus ( $P < .001$ ; Figure 1A). The mean latency of disease onset in *CALM-AF10*-infected mice was 5.5 months; by 9 months of age, all 45 transgenic mice either displayed symptoms of leukemia and were killed (41) or were found dead (4). Necropsy of leukemic mice typically revealed marked lymphadenopathy, hepatosplenomegaly, pale kidneys, and, in some cases, enlarged thymi.

### *CALM-AF10* mice develop B-lineage ALL and AML

*CALM-AF10* mice infected with MOL4070LTR developed either acute lymphoid (B-cell or T-cell), myeloid, biphenotypic (myeloid and B-cell), or biclonal (myeloid and B-cell) leukemia, as determined by histologic and immunophenotypic analysis. Of the 4 mice that were found dead in their cages, 1 mouse did not have evidence of leukemia (mouse 52) and 2 mice (2 and 32) had leukemia by histology, but DNA was degraded and unsuitable for Southern blots or LM-PCR. Therefore, a total of 42 *CALM-AF10* mice infected with MOL4070LTR were available for analysis. Leukemic blasts were typically evident in peripheral blood, spleen, BM, lymph nodes, liver, and kidney. The Bethesda proposals<sup>14,15</sup> were used to classify the leukemias; in some cases, biclonal and biphenotypic diagnoses were applied. Biclonal leukemias represent 2 distinct clones with cell populations that express distinct surface antigens, which are not expressed on cells from the other clone. This is in contrast to biphenotypic leukemias, which are thought to arise in a multipotent progenitor cell capable of differentiating into both myeloid and lymphoid lineages. As shown in Figure 1, of the 42 mice, there was a smaller percentage of pre-T lymphoblastic leukemia/lymphoma (pre-T LBL; 2%), and a larger proportion of

**Table 1. Common integration sites in CALM-AF10 mice infected with the MOL4070LTR retrovirus**

Gene	Incidence	Occurrence in RTCGD*	Mouse ID
<i>Nf1</i>	12†	30	13, 17, 23, 25, 26, 31, 36, 40, 42, 44, 96, 98
<i>Zeb2</i>	11†	14	5, 17, 21, 23, 25, 26, 27, 36, 51, 80, 98
<i>Mn1</i>	6	12	25, 38, 39, 46, 67, 80
<i>Evi1</i>	5	19	6, 14, 29, 31, 36
<i>Mlt3</i>	3	2‡	14, 47, 69
<i>Plag1</i>	2	8	21, 42
<i>Mpl</i>	2	0‡	10, 80
<i>Prkcz</i>	2	0‡	17, 31
<i>CX763467</i>	2	0‡	25, 42
<i>Foxp1</i>	2	1‡	35, 88
<i>Kras</i>	2	8	20, 27
<i>Rras2</i>	2	35	39, 98
<i>Tle3</i>	2	4‡	40, 69
<i>Phb</i>	2	1‡	69, 96
<i>Irf57/Cd47</i>	2	2‡	36, 69
<i>Erg</i>	2	6	6, 69
<i>Vav1</i>	2	0‡	15, 74
<i>Gata1</i>	2	0‡	14, 47
<i>Cybb</i>	2	0‡	40, 8

\*Data from retroviral insertion studies in hematologic malignancies include 2783 total insertions.

†Includes integrations identified by Southern blot analysis.

‡Not previously identified as a common integration site.

B-ALL (29%), biphenotypic (13%), and biclonal leukemias (9%) in CALM-AF10-infected mice compared with WT-infected mice. Leukemic spleens from these mice were also evaluated for clonal *Igh* gene rearrangements; 23 of 42 mice had clonal *Igh* rearrangements (supplemental Figure 1). Taken together, these findings indicate that CALM-AF10 mice infected with retrovirus developed a broader spectrum of leukemic phenotypes than did CALM-AF10 mice not infected with retrovirus, which developed predominantly myeloid leukemia.<sup>5</sup>

#### Clonality of leukemias in CALM-AF10 mice infected with retrovirus

Leukemic samples from infected CALM-AF10 mice were evaluated using Southern blots to determine clonality of the leukemias. As shown in Figure 1, between 1 and 9 integrations per tumor were detected ( $4.4 \pm 0.5$  integrations for the WT mice and  $5.7 \pm 0.5$  integrations for the CALM-AF10 mice,  $P > .05$ ), indicating that the tumors were clonal or oligoclonal, but not polyclonal. These findings suggest several possibilities. A single dominant band (such as mouse 10, Figure 1C) suggests that a clonal leukemia developed from a single integration event. A second pattern was seen in mouse 9 (Figure 1C), which had 5 unique bands, all of equal intensity, suggesting that the leukemia was composed of 1 major clone with 5 insertions. In contrast, mouse 13 developed a leukemia that contains 2 prominent bands and 3 less intense bands; this leukemia is probably oligoclonal, composed of a major clone (represented by the 2 intense bands) and a minor clone (represented by the 3 fainter bands).

#### LM-PCR identifies common retrovirus insertion sites

Using LM-PCR, a total of 262 unique insertions were identified in 40 mice (supplemental Table 2). Nineteen common insertion sites (CISs), defined as 2 or more insertion within a 100-kb window,<sup>17</sup> were identified and are listed in Table 1. Nonrecurrent single integration sites that are of interest because of the function of nearby genes were also noted (supplemental Table 2).

Retroviral integrations were identified within intron 36 of the tumor suppressor gene *Nf1* in 4 mice by LM-PCR (17, 23, 36, and 98). The retroviral integrations determined by LM-PCR were confirmed by Southern blot analysis, and 8 additional integrations were identified (13, 25, 26, 31, 40, 42, 44, and 96, see representative examples in Figure 2A). Of note, there was loss of the germline allele in mice 17 and 23; this reduction to homozygosity, with loss of the WT *Nf1* allele, is similar to the uniparental disomy seen in

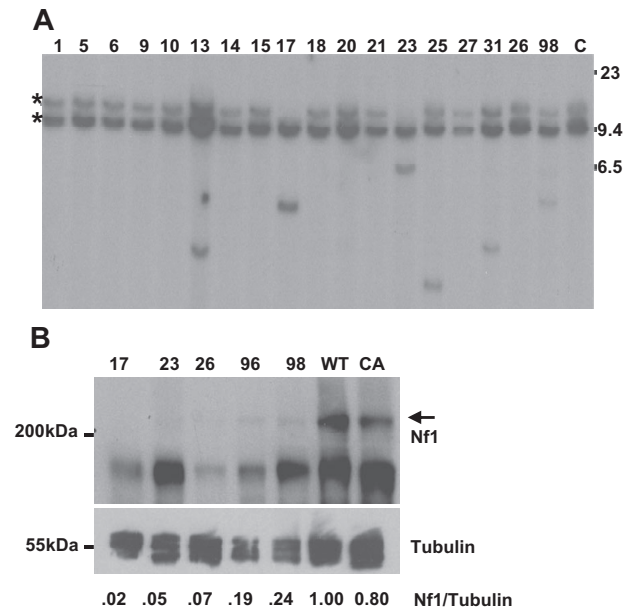


**Figure 2. Nf1 analysis.** (A) Southern blot of *Bam*HI-digested DNA from leukemic spleens hybridized to an *Nf1* probe; 2 germline bands are seen as the probe contains a *Bam*HI site. Mouse identification numbers are indicated; C indicates germline control tissue; size standards are given in kilobases. \*Germline bands. Note loss of the germline allele in mice 17 and 23. (B) Protein lysates from leukemic spleens with a known *Nf1* CIS were compared with spleens from clinically healthy CALM-AF10 and WT mice. The *Nf1* protein is indicated with  $\rightarrow$ ; sizes are in kDa. The blot was reprobed with anti- $\alpha$ -tubulin as a loading control. Intensity of the *Nf1* and  $\alpha$ -tubulin signals were quantified with ImageJ software, and the ratio compared with that of the WT mouse.



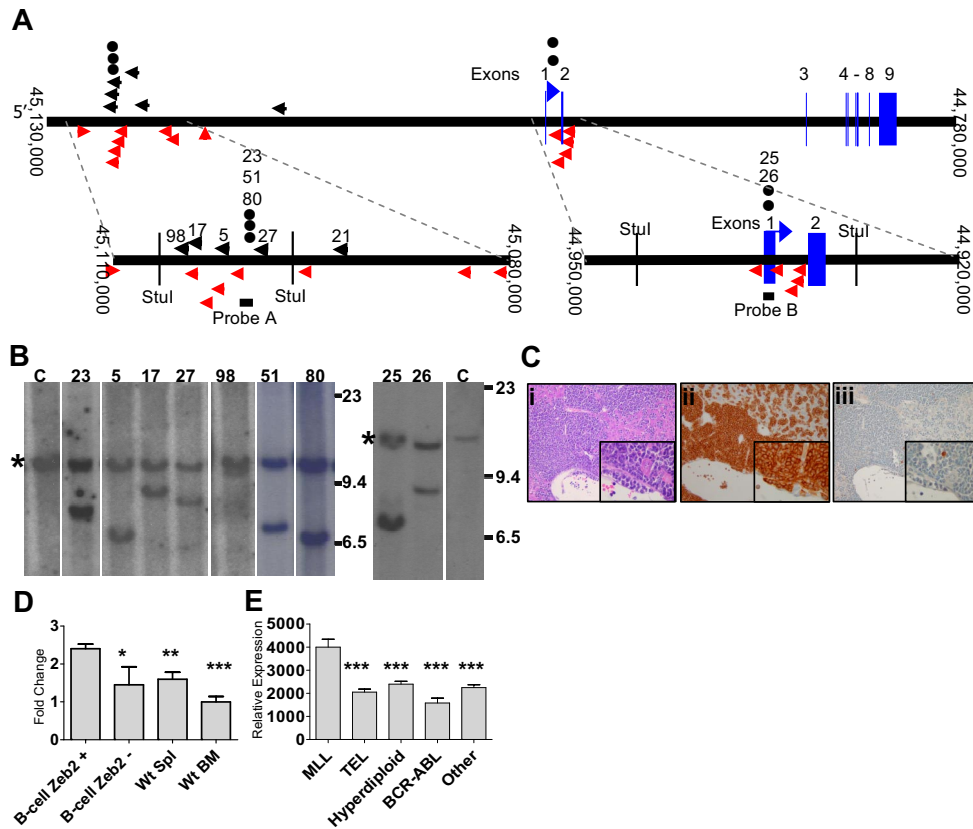


**Figure 3. *Zeb2* integration analysis.** (A) Mouse chromosome 2. Insertions identified by LM-PCR are indicated by black arrows. Insertion events reported in the RTCGD are indicated by red arrows. The vertical red arrow represents an insertion event for which the integration orientation was not reported in the RTCGD. (●) Insertion events identified by Southern blot. Probes A and B are indicated by black bars. Numbers above black arrows and circles represent mice with *Zeb2* integrations. (B) Southern blot of *Stul*-digested genomic DNA from infiltrated spleen hybridized to a *Zeb2* probe. Mouse identifications are indicated; C indicates germline control tissue; size standards are given in kilobases. \*Germline bands. Note the equal intensity of germline and rearranged bands indicating that the leukemias were predominately clonal, except for mouse 98. (C) Acute lymphoid leukemia (B-ALL) in *CALM-AF10* mouse 17 infected with MOL4070LTR. Hematoxylin and eosin-stained liver (Ci inset), B220 stained liver (Cii inset), and myeloperoxidase-stained liver (Ciii inset). (D) mRNA levels determined by quantitative PCR of leukemic spleens with *Zeb2* retrovirus insertions (N = 9). *Zeb2* expression was normalized to the 18S ribosomal control and compared with WT spleen (N = 5 independent samples), WT bone marrow (N = 5 independent samples), or B-lineage ALL samples without *Zeb2* integrations (N = 4, mice 8, 14, 38, and 39). \* $P < .03$ . \*\* $P < .01$ . \*\*\* $P < .001$ . (E) Relative *ZEB2* expression in pediatric B-lineage leukemias determined by expression array from supplemental data reported by Yeoh et al (<http://www.stjudersearch.org/data/ALL1>).<sup>20</sup> Asterisks denote comparison of each group to the *MLL* group; for all comparisons,  $P < .001$ .

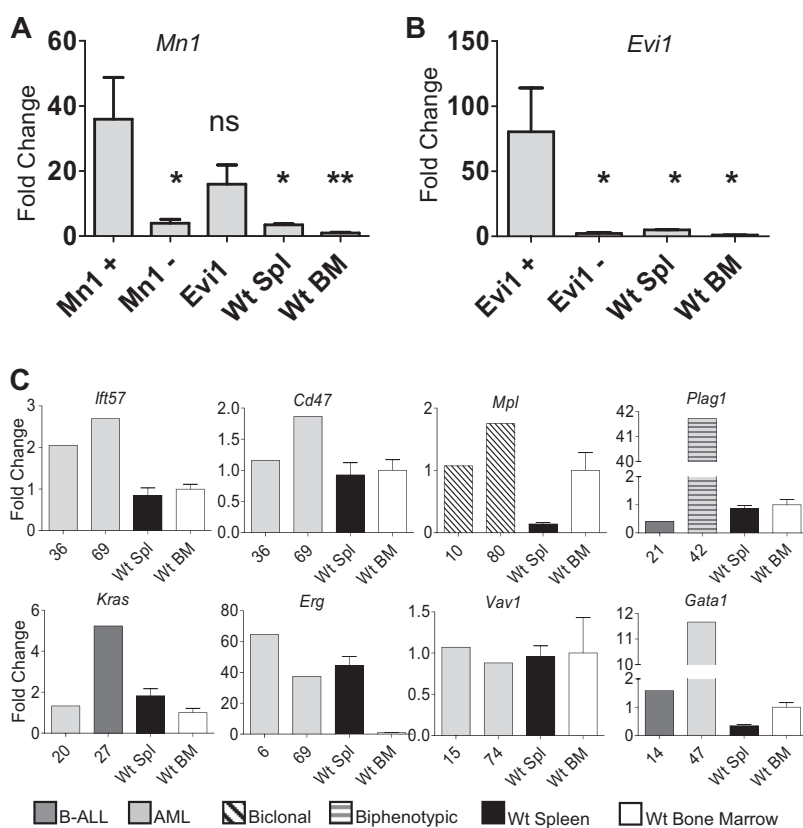
some NF1 patients with AML.<sup>18</sup> Given the known role of *Nf1* as a tumor suppressor gene, the observation that these insertions occurred far away from the *Nf1* promoter, and the loss of the WT allele in some samples, we anticipated that *Nf1* mRNA would be decreased in these mice. However, quantitative RT-PCR assays showed no consistent decrease of *Nf1* mRNA expression in samples with *Nf1* insertions; therefore, we evaluated the expression of Nf1 protein by Western blot in 5 mice with *Nf1* integrations. As shown in Figure 2B, Nf1 protein expression was markedly decreased or absent compared with Nf1 protein expression in either WT or *CALM-AF10* transgenic spleen.

*Zeb2* integrations were identified in 6 *CALM-AF10* mice (5, 17, 21, 27, 36, and 98) by LM-PCR, as indicated in Figure 3A. This gene has been identified 14 times of 2783 retroviral integrations in mouse hematopoietic tumors reported in the Retroviral Tagging Cancer Genome Database (RTCGD; <http://rtcgd.abcc.ncifcrf.gov/>). Five of the 6 *Zeb2* integrations we identified by LM-PCR occurred within a 12-kb cluster 5' of *Zeb2* (Figure 3A). To determine whether the *Zeb2* integrations occurred in a major clone, as well as to identify additional *Zeb2* integrations that might have been missed by LM-PCR, we used Southern blot analysis with a probe from the aforementioned 12-kb cluster (Figure 3A probe A). We were able to confirm the insertion in all 4 mice that had integrations within the range of this assay. In 3 of 4 mice (5, 17, and 27), the

rearranged allele (Figure 3B) was of similar intensity to the germline allele, indicating that the leukemic clone, which contained the *Zeb2* integration was the major, if not sole, leukemic clone in those mice. The *Zeb2* rearranged band from mouse 98 was fainter than the germline band, suggesting that this leukemia represented a minor clone. Three additional leukemias (23, 51, and 80), which had not been identified by LM-PCR, were shown to have *Zeb2* integrations by Southern blot.

Because there was a second, smaller cluster of viral integrations in the RTCGD surrounding the first exon of *Zeb2* (Figure 3A), we speculated that there might be additional integrations in this region that were not identified by LM-PCR. A second Southern blot analysis was performed using a probe that assessed a region encompassing the first exon of *Zeb2*, and 2 additional mice (25 and 26) with *Zeb2* integrations were identified. In sum, 11 of 42 (26%) mice had *Zeb2* integrations, and in 8 of the 9 evaluable cases (integrations for mice 21 and 36 occurred outside of the regions assayed by the probes), the *Zeb2* integration was present in the major leukemic clone. In contrast, we detected only 1 integration (in a very minor clone) in 15 WT mice infected with the MOL4070LTR (supplemental Figure 3), and *Zeb2* integrations have been identified in only 14 of 2783, or less than 0.4%, of the integration sites deposited in the RTCGD ( $P < .001$ ). Ten of 11 (89%) mice with a *Zeb2* integration had B-cell ALL (a

**Figure 4. Increased expression of CIS genes.** (A) Expression levels of *Mn1* were evaluated in mice with *Mn1* insertions (N = 4), mice without *Mn1* or *Evi1* insertions (N = 5), mice with *Evi1* insertions but without *Mn1* insertions (N = 5), WT spleen (N = 5), and WT BM (N = 5). \* $P < .03$ . \*\* $P < .01$ . ns indicates not significant. (B) Expression levels of *Evi1* in mice with *Evi1* insertions (N = 5), mice without *Evi1* insertions (N = 4), WT spleen (N = 5), and WT BM (N = 5). (C) Evaluation of 8 additional CIS (*Plag1*, *Mpl*, *Kras*, *Erg*, *Ift57*, *Cd47*, *Vav1*, and *Gata1*) compared with either WT bone marrow (N = 5) or WT spleen (N = 5). Expression of each gene was determined by quantitative RT-PCR and normalized to the 18S ribosomal RNA.



representative example is shown in Figure 3C) or biphenotypic leukemia with clonal *Igh* gene rearrangements. In contrast, only 13 of 33 (39%) leukemic mice without *Zeb2* integrations had B-cell features (B-cell ALL, biphenotypic, or biclonal;  $P > .004$ ).

Given that the leukemias we detected in this study were B-ALL, AML, biphenotypic, and biclonal leukemias, although BM alone may be a reasonable comparison for myeloid leukemias, it may not be an adequate comparison tissue for B-lineage leukemias. Therefore, in these and subsequent experiments, we present data for both WT BM and spleen as controls. Expression of *Zeb2* in the leukemic samples was 2- to 3-fold higher than in WT spleen, WT BM, or B-lineage leukemias without *Zeb2* integrations (Figure 3D), and there was no difference in *Zeb2* expression between the upstream cluster (mean relative expression, 2.48; N = 7) and the downstream cluster (mean relative expression, 2.13; N = 2). Interestingly, *ZEB2* was also up-regulated in *MLL* rearranged pediatric B-cell precursor ALLs (which, similar to *CALM-AF10* fusions, also overexpress *HOXA* cluster genes) compared with other groups of pediatric B-cell precursor ALL (Figure 3E).<sup>19,20</sup>

Because the upstream cluster of integrations was approximately 140 kb 5' of *Zeb2*, we considered the possibility that integrations at this cluster might affect another gene in addition to *Zeb2*. Based on National Center for Biotechnology Information mouse genome Build 37 (July 2007 Assembly), there was a spliced EST (BB633916) and a noncoding RNA (MMU56439) located near the upstream cluster (supplemental Figure 4A). We could not detect expression of the spliced EST (BB633916) using 4 sets of PCR primers (data not shown). Although the noncoding RNA (MMU56439) was expressed in all samples analyzed, its expression was not significantly higher in samples with *Zeb2* integrations than without *Zeb2* integrations (supplemental Figure 4B). These observations, together with the fact that *Zeb2* mRNA was up-regulated in leukemias from both *Zeb2* integration clusters, as well

as the similarity in leukemic phenotype in mice from both *Zeb2* integration clusters, indicates that *Zeb2* is the target for these integrations.

*Mn1* insertions were identified in 6 mice (25, 38, 39, 46, 67, and 80). Three insertions were located in *Mn1* intron 1, all in the forward direction. These 3 insertions occurred in the same intron as *MN1-TEL* fusions, which have been associated with AML.<sup>21</sup> RT-PCR analysis revealed an in-frame *Mn1-pol* retroviral fusion transcript in all 3 mice with the intron 1 insertion (supplemental Figure 2). This fusion transcript encodes a protein that fuses the *Mn1* N-terminus to the final 115-amino acid residues of the integrase peptide, encoded by the viral *pol* gene (accession no. AAC98548).<sup>16</sup> To determine whether *Mn1* mRNA levels were up-regulated by the insertions, we compared *Mn1* levels in leukemic spleens from mice with *Mn1* insertion to WT BM and spleen. There was a dramatic increase in *Mn1* expression compared with WT spleen or BM (Figure 4A). In addition, we compared *Mn1* levels in leukemic spleens from mice with *Mn1* insertions with those without *Mn1* insertions. As expected, mice without *Mn1* insertions had lower levels of *Mn1* expression, comparable with WT spleen or BM. Interestingly, mice without *Mn1* insertions, but with *Evi1* insertions, also had elevated levels of *Mn1* expression (Figure 4A). These findings are consistent with reports that AML patients with *EVII* overexpression have increased expression of *MN1*.<sup>22</sup>

Five mice (6, 14, 29, 31, and 36) had insertions that were identified within intron 1 of *Evi1*; all of the insertions were determined to be in the opposite orientation of the gene. Four of the 5 mice had a marked increase in *Evi1* mRNA compared with either WT spleen or BM (Figure 4B).

Two mice (36 and 69) had insertions that potentially affected the expression of *Ift57* or *Cd47*. The integrations were 24 or 35 kb 3' of *Ift57* and 66 or 55 kb 5' of *Cd47*. Because these insertions

were located in close proximity to both *Ifr57* and *Cd47*, we considered the possibility that expression of either gene could be influenced by the insertion event. As shown in Figure 4, gene expression for *Ifr57* was elevated in both samples compared with WT spleen and BM, whereas *Cd47* expression was similar to that of WT BM or spleen.

Insertion events 15-kb 5' of *Plagl1* were identified in 2 mice (21 and 42), and there was a 40-fold increase in *Plagl1* expression for mouse 42 compared with WT BM or spleen (Figure 4). Two mice (10 and 80) were identified with insertion events 631 or 933 bp 5' of the thrombopoietin receptor, *Mpl*, and were associated with modest increases in *Mpl* mRNA (Figure 4). *Kras* was identified as a CIS in 2 mice (20 and 27) and was up-regulated in 1 of the 2 mice (27, Figure 4). Retroviral insertions in the second intron of *Erg* were identified in 2 mice (6 and 69) and were associated with a 40- to 60-fold mRNA increase compared with WT BM (Figure 4). Two mice (14 and 47) had *Gatal* insertions, either within the first intron (mouse 14) or 2.7 kb 5' of the transcript initiation site (mouse 47); *Gatal* expression was markedly elevated in mouse 47 (Figure 4).

*Meis1* has commonly been identified by RIM, and *Meis1* insertions were identified in 13 of 32 samples in a previous study using the MOL4070LTR virus.<sup>16</sup> However, only a single *Meis1* insertion was identified in this current study. Therefore, we screened the 42 leukemia samples for *Meis1* insertion using Southern blot analysis, as previously described,<sup>16</sup> but no additional *Meis1* insertions were identified (data not shown).

#### ZEB2 knockdown leads to decreased proliferation of the MV4-11 cell line

Because we know of no B-lineage cell lines that express a *CALM-AF10* fusion, we studied MV4-11 cells,<sup>23</sup> a human B-cell precursor ALL cell line that expresses an *MLL-AF4* fusion, which, similar to the *CALM-AF10* fusion, leads to up-regulation of *HoxA9* and *MEIS1*, as a surrogate. To assess off-target effects of the *ZEB2* siRNA in human B cells, MV4-11 cells were compared with B-ALL1 cells,<sup>24</sup> a human B-cell precursor ALL cell line that does not express an *MLL-AF4* fusion. Similar to the results shown in Figure 3E, *ZEB2* was markedly overexpressed in MV4-11 cells compared with BALL-1 cells (Figure 5A). We used a *ZEB2* siRNA to inhibit expression of *ZEB2* in the MV4-11 cells, leading to decreased proliferation of MV4-11 cells, but not B-ALL1 cells, suggesting that ongoing *ZEB2* expression was important for proliferation of the MV4-11 cells, but not the B-ALL1 cells (Figure 5B-C).

#### Ras pathway resequencing identifies spontaneous mutations

We hypothesized that the frequent *Nf1* insertion resulted in Ras pathway activation. Given that point mutations of *NRAS*, *KRAS*, *PTPN11*, or *FLT3* are common in AML<sup>25</sup> and ALL<sup>26</sup> patients, we evaluated *CALM-AF10* retroviral-infected leukemic mice for spontaneous activating mutations in these genes. We sequenced *Nras* and *Kras* exons 2/3 in all 42 mice and found 2 mutations: a codon 12 GGT to GAT (Gly to Asp) mutation in mouse 25 and a codon 13 GGT to GAT (Gly to Asp) mutation in mouse 27 (Table 2). We also sequenced *Ptpn11* exon 3 and *Flt3* exon 20 in all 42 mice. We found 1 spontaneous point mutation in *Ptpn11* exon 3 in mouse 5 (supplemental Figure 5), a codon 72 GCC to GTC (Ala to Val) mutations, which has also been found in human ALL,<sup>26</sup> AML,<sup>27</sup> and juvenile myelomonocytic leukemia (JMML).<sup>28</sup> No spontaneous point mutations were found in the tyrosine kinase

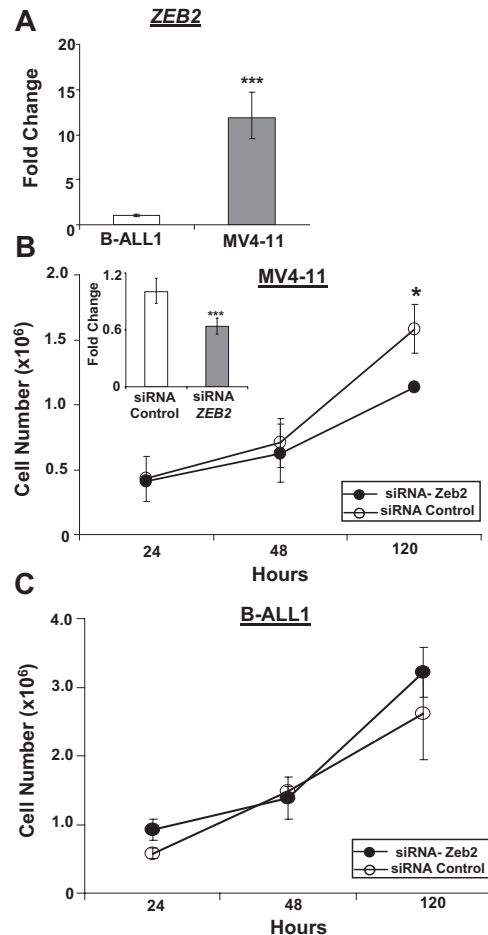


**Figure 5. Inhibition of *ZEB2* leads to decreased proliferation of MV4-11 cells.** (A) Expression of *ZEB2* mRNA in MV4-11 and B-ALL1 cell lines. (B) Inhibition of *ZEB2* mRNA expression in MV4-11 cell line by siRNA leads to decreased proliferation. (Inset) *ZEB2* quantitative RT-PCR assay at 24 hours. (C) Treatment of B-ALL1 cell line with *ZEB2* siRNA does not lead to decreased proliferation. Quantitative RT-PCR values are plotted as minimum/maximum values from triplicate assays. \* $P < .03$ . \*\*\* $P < .001$ . Error bars for 120-hour *Zeb2* siRNA time point are very small and not visible.

domain of *Flt3*. Remarkably, all of the Ras pathway point mutations occurred in mice with *Zeb2* insertions. In total, 8 of 11 mice with *Zeb2* insertions also had *Nf1* insertions or Ras pathway activating mutations, whereas only 6 of 31 mice without *Zeb2* insertions had *Nf1* insertions, and none of these mice had point mutations. This difference was highly significant ( $P < .003$ ; Table 2).

## Discussion

*CALM-AF10* transgenic mice develop leukemia after a long latency period with incomplete penetrance, suggesting the need for complementary events.<sup>5</sup> In contrast, infection of mouse BM with a *CALM-AF10* retrovirus led to AML in 100% of mice after a short latency.<sup>4</sup> The AMLs in that study were clonal, as demonstrated by clonal *Igh* gene rearrangements, suggesting the possibility that a cooperative event had been introduced by the retrovirus used to carry the *CALM-AF10* cDNA. Although the authors did not detect any CIS among the 18 retroviral insertions cloned in that study, it remains possible that collaborating insertions were not identified, or that the insertions identified, even though not known CIS,

**Table 2. *Nf1* insertions and *Ras* pathway mutations in *CALM-AF10* mice with *Zeb2* insertions**

ID	Diagnosis	IgH rearrangement	Proviral insertion	Gene mutation
5	B-ALL	Yes	—	<i>Ptpn11</i>
17	B-ALL	Yes	<i>Nf1</i>	—
21	B-ALL	Yes	—	—
23	B-ALL	Yes	<i>Nf1</i>	—
25	B-ALL	Yes	<i>Nf1</i>	<i>Kras</i>
26	B-ALL	Yes	<i>Nf1</i>	—
27	B-ALL	Yes	—	<i>Kras</i>
36	AML	No	<i>Nf1</i>	—
51	Biphenotypic	Yes	—	—
80	Biphenotypic	Yes	—	—
98	B-ALL	Yes	<i>Nf1</i>	—

Eight of 11 mice with *Zeb2* insertions also had *Nf1* insertions and/or *Ras* pathway activating point mutations. Only 6 of 31 mice without *Zeb2* insertions have *Nf1* insertions, and none of these mice had *Ras* pathway activating point mutations ( $P < .003$ ).

— indicates no *Nf1* insertion or gene mutation was identified.

collaborated with the *CALM-AF10* fusion to produce AML. We used retroviral insertional mutagenesis to identify candidate genes that could complement a *CALM-AF10* fusion.

The most common retroviral integration in *CALM-AF10* mice was located within intron 36 of *Nf1*. Neurofibromatosis type 1 is an autosomal disorder caused by inactivating mutations of *NF1*.<sup>29</sup> Children with NF1 are at increased risk for developing malignant myeloid disease, including AML and JMML, which is often associated with monosomy 7, suggesting a collaboration between monosomy 7 and NF1.<sup>30,31</sup> *NF1* encodes a protein that serves as a GTPase-activating protein which accelerates Ras-GTP hydrolysis, converting Ras-GTP to its inactive form Ras-GDP.<sup>32</sup> Several lines of evidence emphasize the role of *Nf1* as a tumor suppressor gene. *Nf1*<sup>+/-</sup> heterozygous mice developed a myeloproliferative disease, in year 2 of life, which was associated with LOH at the *Nf1* locus in myeloid cells,<sup>33</sup> similar to findings in patients with JMML. Transplantation of *Nf1*<sup>-/-</sup> fetal liver cells leads to a myeloproliferative syndrome that resembles JMML.<sup>34</sup> Finally, analysis of retroviral integration sites in BXH2 mice that developed leukemias identified common integrations within *Nf1* intron 36, often with loss of Nf1 protein expression.<sup>35</sup>

In the current series, *Nf1* was identified as a CIS in 12 of 42 mice. The leukemic cells from 2 mice (17 and 23) demonstrated loss of the germline *Nf1* allele, consistent with the known role of *Nf1* as a tumor suppressor gene. Similar to previous reports, although *Nf1* mRNA expression was consistently detected in mice with *Nf1* insertions, *Nf1* protein expression was absent or markedly decreased. Given the frequent association of *NF1* gene inactivation and monosomy 7, which itself is associated with marked overexpression of *HOXA9*,<sup>36</sup> it is interesting to note that *Hoxa9* expression is also markedly elevated in BM from *CALM-AF10* mice,<sup>5</sup> supporting the hypothesis that *Nf1* inactivation collaborates with *Hoxa9* gene activation.

*Zeb2* (*Sip1* or *Zfhx1b*) was identified as a CIS in 11 of 42 mice. However, *Zeb2* has only rarely been identified in previous RIM studies and has not previously been implicated in leukemic transformation. Much of what is known about *ZEB2* function stems from studies in patients with Mowat-Wilson syndrome,<sup>37</sup> a developmental disorder of neural crest-derived tissue that results from germline mutations of *ZEB2*.<sup>38</sup> Interestingly, several lines of evidence are consistent with the hypothesis that *ZEB2* may be involved in malignant transformation. The *ZEB2* protein interacts with several members of the SMAD protein family, including SMAD1, SMAD2, SMAD3, and SMAD5<sup>39</sup>; SMAD proteins have been shown to play important roles in normal and malignant hematopoiesis.<sup>40</sup> In addition, *Zeb2* has been shown to act upstream

of Wnt signaling,<sup>41</sup> and recent evidence implicates Wnt signaling in hematopoietic stem cell self-renewal and progenitor development,<sup>42</sup> including B lymphocyte proliferation.<sup>43</sup> Furthermore, overexpression of *ZEB2* in primary epithelial cells promotes epithelial-mesenchymal transition, a transdifferentiation process observed in breast cancer and renal cell carcinoma.<sup>44</sup> Finally, a preliminary report indicated that *ZEB2* was overexpressed in leukemia patients with *MLL* gene rearrangements.<sup>45</sup>

*Zeb2* integrations were present in the dominant leukemic clone in most of the mice with this CIS. In addition, mouse 5 had a single retroviral integration in the dominant clone (Figure 1); this integration involved *Zeb2* (Figure 3), strongly suggesting that the *Zeb2* integrations were important for leukemic transformation, and were not merely “passengers.” Furthermore, we noted that most of the mice with *Zeb2* insertions developed B-cell or biphenotypic leukemia, suggesting that *Zeb2* collaborates with *CALM-AF10* to promote B-cell leukemia. The only mouse (36) that had neither a B-cell phenotype nor a clonal *Igh* gene rearrangement did not overexpress *Zeb2*, and had an integration site outside of the region assayed by either of the Southern blot probes. Therefore, it is possible that the leukemic clone containing a *Zeb2* integration from mouse 36 represented a minor clone, or that integration outside of the 2 clusters did not lead to overexpression of *Zeb2*. The mice with *Zeb2* integrations had increased expression of *Zeb2* at the mRNA level compared with WT spleen. Increased expression of *ZEB2* is also present in pediatric ALLs with rearranged *MLL* compared with other pediatric ALLs. The high incidence of *Zeb2* insertions in our *CALM-AF10* model and the consistent overexpression of *ZEB2* in *MLL* rearranged ALLs suggest that increased *ZEB2* may collaborate with *HOXA9/MEIS1* overexpression in ALL patients.

*Mn1* was identified 6 times as a CIS. *MN1* forms a fusion transcript with *TEL* in some AML patients,<sup>21</sup> and *MN1* overexpression is associated with a poor response to induction chemotherapy, increased relapse rate, and decreased overall survival.<sup>46</sup> In addition, *Mn1* was reported as a CIS in *NUP98-HOXD13* transgenic mice, which overexpress *Hoxa7*, *9*, and *10* in the BM, and a *MN1-TEL* fusion has been shown to collaborate with *HOXA9* to induce AML in a murine BM transplantation model.<sup>47</sup> Given that *Hoxa9* is up-regulated in *CALM-AF10* mouse BM, these findings collectively suggest a collaborative role between overexpression of *Hoxa9* and *Mn1* in leukemic transformation.

Activating point mutations in *Ras* pathway genes developed spontaneously in mice with 2 additional oncogenic events (*CALM-AF10* transgene and retroviral insertion), reinforcing the importance of *Ras* pathway activation in leukemogenesis. In addition, there is a remarkably strong correlation between *Ras* pathway



activation, via *Nfl* inactivation or spontaneous point mutation (*Kras* or *Ptpn11*), and *Zeb2* activation via proviral integration in our study.

Of note, we did not identify a CIS near *Meis1*, a transcription factor that collaborates with *HOX* genes during leukemic transformation.<sup>48,49</sup> *Meis1* has often been identified as a CIS through a retroviral mutagenesis screen in mice<sup>50</sup> and was identified as a CIS in 14 of 32 *NUP98HOXD13* transgenic mice that were infected with the MOL4070LTR.<sup>16</sup> However, we previously demonstrated that *Meis1* was markedly overexpressed in BM from *CALM-AF10* mice.<sup>5</sup> Therefore, there may be no selective advantage for *Meis1* insertions in *CALM-AF10* mice because *CALM-AF10* mice without *Meis1* insertions overexpress *Meis1*.

Although *CALM-AF10* fusions are rare, these translocations share many important biologic features with *MLL* fusions, including a tendency to produce both myeloid and lymphoid malignancy. Using retroviral insertional mutagenesis and targeted resequencing, we have identified potential collaborative oncogenic pathways that complement *CALM-AF10* fusions, and, by extension, similar translocations during leukemic transformation. The frequent correlation of *Zeb2* integrations and *Ras* pathway activating mutations in *CALM-AF10* mice suggests that *Zeb2* and *Ras* pathway activation collaborate with *CALM-AF10* (and potentially other leukemic fusions that activate *HOXA* cluster genes) to induce leukemia.

## References

- Bohlander SK, Muschinsky V, Schrader K, et al. Molecular analysis of the CALM/AF10 fusion: identical rearrangements in acute myeloid leukemia, acute lymphoblastic leukemia and malignant lymphoma patients. *Leukemia*. 2000;14(1):93-99.
- Dreyling MH, Martinez-Climent JA, Zheng M, Mao Y, Rowley JD, Bohlander SK. The t(10;11)(p13;q14) in the U937 cell line results in the fusion of the AF10 gene and CALM, encoding a new member of the AP-3 clathrin assembly protein family. *Proc Natl Acad Sci U S A*. 1996;93(10):4804-4809.
- Kobayashi H, Hosoda F, Maseki N, et al. Hematologic malignancies with the t(10;11)(p13;q21) have the same molecular event and a variety of morphologic or immunologic phenotypes. *Genes Chromosomes Cancer*. 1997;20(3):253-259.
- Deshpande AJ, Cusan M, Rawat VP, et al. Acute myeloid leukemia is propagated by a leukemic stem cell with lymphoid characteristics in a mouse model of CALM/AF10-positive leukemia. *Cancer Cell*. 2006;10(5):363-374.
- Caudell D, Zhang Z, Chung YJ, Aplan PD. Expression of a CALM-AF10 fusion gene leads to Hoxa cluster overexpression and acute leukemia in transgenic mice. *Cancer Res*. 2007;67(17):8022-8031.
- Kelly LM, Gilliland DG. Genetics of myeloid leukemias. *Annu Rev Genomics Hum Genet*. 2002;3:179-198.
- Mathew S, Raimondi SC. FISH, CGH, and SKY in the diagnosis of childhood acute lymphoblastic leukemia. *Methods Mol Biol*. 2003;220:213-233.
- Armstrong SA, Look AT. Molecular genetics of acute lymphoblastic leukemia. *J Clin Oncol*. 2005;23(26):6306-6315.
- Suzuki T, Shen H, Akagi K, et al. New genes involved in cancer identified by retroviral tagging. *Nat Genet*. 2002;32(1):166-174.
- Uren AG, Kool J, Berns A, van Lohuizen M. Retroviral insertional mutagenesis: past, present and future. *Oncogene*. 2005;24(52):7656-7672.
- Palmqvist L, Pineault N, Wasslavik C, Humphries RK. Candidate genes for expansion and transformation of hematopoietic stem cells by NUP98-HOX fusion genes. *PLoS One*. 2007;2(1):e768.
- Harper DP, Aplan PD. Chromosomal rearrangements leading to MLL gene fusions: clinical and biological aspects. *Cancer Res*. 2008;68(24):10024-10027.
- Wolff L, Koller R, Hu X, Anver MR. A Moloney murine leukemia virus-based retrovirus with 4070A long terminal repeat sequences induces a high incidence of myeloid as well as lymphoid neoplasms. *J Virol*. 2003;77(8):4965-4971.
- Kogan SC, Ward JM, Anver MR, et al. Bethesda proposals for classification of nonlymphoid hematopoietic neoplasms in mice. *Blood*. 2002;100(1):238-245.
- Morse HC 3rd, Anver MR, Fredrickson TN, et al. Bethesda proposals for classification of lymphoid neoplasms in mice. *Blood*. 2002;100(1):246-258.
- Slape C, Hartung H, Lin YW, Bies J, Wolff L, Aplan PD. Retroviral insertional mutagenesis identifies genes that collaborate with NUP98-HOXD13 during leukemic transformation. *Cancer Res*. 2007;67(11):5148-5155.
- Mikkers H, Allen J, Knipscheer P, et al. High-throughput retroviral tagging to identify components of specific signaling pathways in cancer. *Nat Genet*. 2002;32(1):153-159.
- Stephens K, Weaver M, Leppig KA, et al. Interstitial uniparental isodisomy at clustered breakpoint intervals is a frequent mechanism of NF1 inactivation in myeloid malignancies. *Blood*. 2006;108(5):1684-1689.
- Ross ME, Zhou X, Song G, et al. Classification of pediatric acute lymphoblastic leukemia by gene expression profiling. *Blood*. 2003;102(8):2951-2959.
- Yeoh EJ, Ross ME, Shurtleff SA, et al. Classification, subtype discovery, and prediction of outcome in pediatric acute lymphoblastic leukemia by gene expression profiling. *Cancer Cell*. 2002;1(2):133-143.
- Buijs A, Sherr S, van Baal S, et al. Translocation (12;22)(p13;q11) in myeloproliferative disorders results in fusion of the ETS-like TEL gene on 12p13 to the MN1 gene on 22q11. *Oncogene*. 1995;10(8):1511-1519.
- Valk PJ, Verhaak RG, Beijnen MA, et al. Prognostically useful gene-expression profiles in acute myeloid leukemia. *N Engl J Med*. 2004;350(16):1617-1628.
- Lange B, Valtieri M, Santoli D, et al. Growth factor requirements of childhood acute leukemia: establishment of GM-CSF-dependent cell lines. *Blood*. 1987;70(1):192-199.
- Hiraki S, Miyoshi I, Masuji H, Kubonishi I, Matsuda Y. Establishment of an Epstein-Barr virus-determined nuclear antigen-negative human B-cell line from acute lymphoblastic leukemia. *J Natl Cancer Inst*. 1977;59(1):93-94.
- Renneville A, Roumier C, Biggio V, et al. Co-operating gene mutations in acute myeloid leukemia: a review of the literature. *Leukemia*. 2008;22(5):915-931.
- Paulsson K, Horvat A, Strombeck B, et al. Mutations of FLT3, NRAS, KRAS, and PTPN11 are frequent and possibly mutually exclusive in high hyperdiploid childhood acute lymphoblastic leukemia. *Genes Chromosomes Cancer*. 2008;47(1):26-33.
- Loh ML, Reynolds MG, Vattikuti S, et al. PTPN11 mutations in pediatric patients with acute myeloid leukemia: results from the Children's Cancer Group. *Leukemia*. 2004;18(11):1831-1834.
- Kratz CP, Niemeyer CM, Castleberry RP, et al. The mutational spectrum of PTPN11 in juvenile myelomonocytic leukemia and Noonan syndrome/myeloproliferative disease. *Blood*. 2005;106(6):2183-2185.
- Korf BR. Malignancy in neurofibromatosis type 1. *Oncologist*. 2000;5(6):477-485.
- O'Marcaigh AS, Shannon KM. Role of the NF1 gene in leukemogenesis and myeloid growth control. *J Pediatr Hematol Oncol*. 1997;19(6):551-554.
- Tefferi A, Gilliland DG. Oncogenes in myeloproliferative disorders. *Cell Cycle*. 2007;6(5):550-566.
- Braun BS, Shannon K. Targeting Ras in myeloid leukemias. *Clin Cancer Res*. 2008;14(8):2249-2252.
- Jacks T, Shih TS, Schmitt EM, Bronson RT, Bernards A, Weinberg RA. Tumour predisposition in mice heterozygous for a targeted mutation in Nf1. *Nat Genet*. 1994;7(3):353-361.
- Largaespada DA, Brannan CI, Jenkins NA,

## Acknowledgments

The authors thank Helge Hartung, Sarah Beachy, Sheryl Gough, Yang Jo Chung, R. Mark Simpson, and Siba Samal for insightful discussions and Christine Perella for expert technical assistance with mouse retroviral infection and necropsies.

This work was supported by the Intramural Research Program of the National Institutes of Health, National Cancer Institute.

## Authorship

Contribution: D.C. and D.P.H. designed and performed research, analyzed data, and wrote the initial drafts of the manuscript; R.L.N., R.M.P., and C.S. designed and performed research and analyzed data; L.W. designed research and supervised the retroviral infections; and P.D.A. designed research, analyzed data, and wrote the final draft of the manuscript.

Conflict-of-interest disclosure: The authors declare no competing financial interests.

Correspondence: Peter D. Aplan, NIH/NCI/CCR/Genetics Branch, 8901 Wisconsin Ave, Navy 8, Rm 5101, Bethesda, MD 20889-5105; e-mail: aplan@mail.nih.gov.

- Copeland NG. Nf1 deficiency causes Ras-mediated granulocyte/macrophage colony stimulating factor hypersensitivity and chronic myeloid leukaemia. *Nat Genet.* 1996;12(2):137-143.
35. Largaespada DA, Shaughnessy JD Jr, Jenkins NA, Copeland NG. Retroviral integration at the Evi-2 locus in BXH-2 myeloid leukemia cell lines disrupts Nf1 expression without changes in steady-state Ras-GTP levels. *J Virol.* 1995;69(8):5095-5102.
  36. Chen G, Zeng W, Miyazato A, et al. Distinctive gene expression profiles of CD34 cells from patients with myelodysplastic syndrome characterized by specific chromosomal abnormalities. *Blood.* 2004;104(13):4210-4218.
  37. Mowat DR, Wilson MJ, Goossens M. Mowat-Wilson syndrome. *J Med Genet.* 2003;40(5):305-310.
  38. Dastot-Le Moal F, Wilson M, Mowat D, Collot N, Niel F, Goossens M. ZFH1B mutations in patients with Mowat-Wilson syndrome. *Hum Mutat.* 2007;28(4):313-321.
  39. van Grunsven LA, Schellens A, Huylebroeck D, Verschueren K. SIP1 (Smad interacting protein 1) and deltaEF1 (delta-crystallin enhancer binding factor) are structurally similar transcriptional repressors. *J Bone Joint Surg Am.* 2001;83[suppl 1]:S40-S47.
  40. Isufi I, Seetharam M, Zhou L, et al. Transforming growth factor-beta signaling in normal and malignant hematopoiesis. *J Interferon Cytokine Res.* 2007;27(7):543-552.
  41. Miquelajauregui A, Van de Putte T, Polyakov A, et al. Smad-interacting protein-1 (Zfhx1b) acts upstream of Wnt signaling in the mouse hippocampus and controls its formation. *Proc Natl Acad Sci U S A.* 2007;104(31):12919-12924.
  42. Khan NI, Bendall LJ. Role of WNT signaling in normal and malignant hematopoiesis. *Histol Histopathol.* 2006;21(7):761-774.
  43. Reya T, O'Riordan M, Okamura R, et al. Wnt signaling regulates B lymphocyte proliferation through a LEF-1 dependent mechanism. *Immunity.* 2000;13(1):15-24.
  44. Beltran M, Puig I, Pena C, et al. A natural antisense transcript regulates Zeb2/Sip1 gene expression during Snail1-induced epithelial-mesenchymal transition. *Genes Dev.* 2008;22(6):756-769.
  45. Jo A, Tsukimoto I, Ishii E, et al. Age-associated difference in gene expression of pediatric myelomonocytic and MLL-rearranged AML. *ASH Annual Meeting Abstracts.* 2007;110(11):3164.
  46. Heuser M, Beutel G, Krauter J, et al. High menin-gioma 1 (MN1) expression as a predictor for poor outcome in acute myeloid leukemia with normal cytogenetics. *Blood.* 2006;108(12):3898-3905.
  47. Kawagoe H, Grosveld GC. Conditional MN1-TEL knock-in mice develop acute myeloid leukemia in conjunction with overexpression of HOXA9. *Blood.* 2005;106(13):4269-4277.
  48. Moskow JJ, Bullrich F, Huebner K, Daar IO, Buchberg AM. Meis1, a PBX1-related homeobox gene involved in myeloid leukemia in BXH-2 mice. *Mol Cell Biol.* 1995;15(10):5434-5443.
  49. Kroon E, Kros J, Thorsteinsdottir U, Baban S, Buchberg AM, Sauvageau G. Hoxa9 transforms primary bone marrow cells through specific collaboration with Meis1a but not Pbx1b. *EMBO J.* 1998;17(13):3714-3725.
  50. Iwasaki M, Kuwata T, Yamazaki Y, et al. Identification of cooperative genes for NUP98-HOXA9 in myeloid leukemogenesis using a mouse model. *Blood.* 2005;105(2):784-793.